BIOCHEMISTRY
including biophysical chemistry & molecular biology

Article

pubs.acs.org/biochemistry

Structural and Biochemical Characterization of a Ferredoxin:Thioredoxin Reductase-like Enzyme from *Methanosarcina acetivorans*

Adepu K. Kumar,[†,§] R. Siva Sai Kumar,[†] Neela H. Yennawar,[‡] Hemant P. Yennawar,*[,†] and James G. Ferry*[,†]

[†]Department of Biochemistry and Molecular Biology, Pennsylvania State University, University Park, Pennsylvania 16802, United States

[‡]Huck Institutes of Life Sciences, Pennsylvania State University, University Park, Pennsylvania 16802, United States

Supporting Information

ABSTRACT: Bioinformatics analyses predict the distribution in nature of several classes of diverse disulfide reductases that evolved from an ancestral plant-type ferredoxin:thioredoxin reductase (FTR) catalytic subunit to meet a variety of ecological needs. *Methanosarcina acetivorans* is a methane-producing species from the domain Archaea predicted to encode an FTR-like enzyme with two domains, one resembling the FTR catalytic subunit and the other containing a rubredoxin-like domain replacing the variable subunit of present-day FTR enzymes. *M. acetivorans* is of special interest as it was recently proposed to have evolved at the time of the end-Permian extinction and to be largely responsible for the most severe biotic crisis in the fossil record by converting acetate to methane. The crystal structure and biochemical characteristics were determined for the FTR-like enzyme from *M. acetivorans*, here named FDR (ferredoxin disulfide reductase). The results support a role for the rubredoxin-like center of FDR in transfer of electrons from ferredoxin to the active-site [Fe_4S_4] cluster adjacent to a pair of redox-active cysteines participating in reduction of disulfide substrates. A mechanism is proposed for disulfide reduction similar to one of two mechanisms previously proposed for the plant-type FTR. Overall, the results advance the biochemical and evolutionary understanding of the FTR-like family of enzymes and the conversion of acetate to methane that is an essential link in the global carbon cycle and presently accounts for most of this greenhouse gas that is biologically generated.

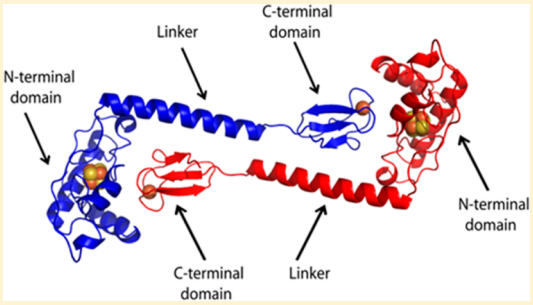

Disulfide reductases are ubiquitous in nature where they interact with protein and small molecule substrates required for diverse physiological functions, including redox regulation and the response to oxidative stress among others. Disulfide reductases belong to a large family of NAD(P)H-dependent flavoenzymes, many of which are well-characterized, including thioredoxin reductases.[1,2] The family employs an active-site dithiol−disulfide to transfer reducing equivalents from the flavin to the substrate. However, the discovery of two novel disulfide reductases has disrupted the paradigm of obligatory two-electron redox reactions involving NADPH and flavins. The plant-type ferredoxin:thioredoxin reductase (FTR) and heterodisulfide reductase (HDR) from methane-producing organisms of the domain Archaea have emerged as unusual disulfide reductases involving an active-site [Fe_4S_4] cluster.[3,4]

Phylogenetic analyses of genomic sequences revealed that the catalytic subunit of FTR originated in deeply rooted microaerophilic species from the domain Bacteria where it appears to have functioned in regulating CO_2 fixation.[2] The analyses further suggest that FTR was acquired by later-evolving species via horizontal gene transfer that evolved FTR-like enzymes with structural and functional diversity to meet ecological needs. For example, the analyses showed that late-evolving species from the domains Bacteria and Archaea contain an FTR-like enzyme with a plant-type FTR catalytic domain in the N-terminal region and a bacterial-like rubredoxin-containing domain in the C-terminal region. The methane-producing archaeon *Methanosarcina acetivorans* was identified as one of the species encoding this FTR-like enzyme.[2] Indeed, Rothman et al.[5] recently concluded that *M. acetivorans* evolved late, at the time of the end-Permian extinction, and that species like it were responsible for the most severe biotic crisis in the fossil record by converting acetate to methane. The biological formation of methane from acetate is an essential link in the present-day global carbon cycle and is the major biological source of this important greenhouse gas.

Although many thioredoxins and thioredoxin reductases are well-characterized in species from the domains Bacteria and Eukarya, the understanding of their functions, structures, and mechanisms in the domain Archaea is limited.[6−10] It was

Received: February 9, 2015
Revised: April 26, 2015
Published: April 27, 2015

DOI: 10.1021/acs.biochem.5b00137
Biochemistry 2015, 54, 3122−3128

recently proposed that these enzymes function in complex regulatory networks of methane-producing species.[2,10] Only three thioredoxin reductases from the domain Archaea have been characterized, all of which belong to the canonical NADP-dependent flavin-containing family.[11−13] Accordingly, it is of significant interest to determine the structure and biochemical properties of FTR-like disulfide reductases to understand their evolution and function. Here we report the crystal structure and biochemical characterization of the FTR-like enzyme FDR (ferredoxin disulfide reductase) from *M. acetivorans*. The results advance the biochemical and evolutionary understanding of the FTR-like novel disulfide reductase family and the conversion of acetate to methane.

MATERIALS AND METHODS

Materials. Ferredoxin (FDX) and ferredoxin-NADP$^+$ reductase (FNR) from *Spinacia oleracea*, NADPH, thioredoxin from *Escherichia coli*, and insulin from bovine pancreas were obtained from Sigma-Aldrich (St. Louis, MO). All other chemicals used were of analytical grade.

Protein Purification. His-tagged FDR was produced in *E. coli* and purified as previously described, except for biochemical investigations in which it was purified anaerobically in a glovebag (Coy Laboratory Products, Ann Arbor, MI) with an inert atmosphere of 95% nitrogen and 5% hydrogen.[14] Purified preparations showed a single prominent band upon being analyzed by 12% sodium dodecyl sulfate−polyacrylamide gel electrophoresis. The 2[Fe_4S_4] FDX from acetate-grown cells of *M. acetivorans* was purified to electrophoretic homogeneity as previously described.[15] Thioredoxin from *M. acetivorans* was produced in *E. coli* and purified to electrophoretic homogeneity as described in the Supporting Information.

Analytical. Protein concentrations were determined by measuring the absorbance at 280 nm of solutions using a theoretical monomer extinction coefficient of 26525 cm^{-1} M^{-1} and a computed monomer molecular mass of 20192 Da. Iron analyses were performed as described previously.[16] The previously described FDX-regenerating system was used in experiments requiring FDX-dependent reduction of FDR.[15] For the assay of continuous GSSG reducing activity, the 1.0 mL reaction mixture contained 0.15 mM FDR, 4.0 μM *M. acetivorans* 2[Fe_4S_4] FDX, 20 mM NADPH, 2 μg of FNR, and 1 mM GSSG in 20 mM HEPES (pH 7.5). An aliquot of the reaction mixture was taken at various time intervals and filtered using centrifugal filter units (3 kDa molecular mass cutoff) to remove FDR. GSH in the filtrate was determined with Ellman's reagent as described previously.[15]

X-ray Crystallography. Crystals, as reported previously,[14] were grown using the sitting drop method at 21 °C and at a protein concentration of 20 mg mL^{-1}. The reservoir well contained 50 mM HEPES buffer (pH 7.5) and 1.7 M ammonium sulfate. Four microliters each of the protein and reservoir were mixed to make the sitting drop. Brown-colored cubical crystals grew in ∼3 weeks. They belonged to cubic space group *P*23 with the following unit cell dimensions: $a = b = c = 93.18$ Å.

Prior to data collection, crystals of FDR were transferred to a cryoprotectant solution containing fructose [55% (v/v)] in mother liquor and also in different heavy atom solutions as described below. Diffraction data were collected on a Quantum 270 detector at the F2 beamline of the Cornell High Energy Synchrotron Source (CHESS). We located the [Fe_4S_4] cluster and obtained an initial set of phases using the single anomalous diffraction (SAD) technique. Further automated model building was feasible in the Phenix suite, and the software was able to build most of the secondary structure.[17] Structural refinement produced a higher resolution of 2.35 Å, collected on a crystal that was also soaked for 2 min in 0.5 M NaBr. Seven bromine sites (the occupancies of six of them were at 0.5 and one at 1.0) balanced by four sodium atoms (all at full occupancy) were identified in this data set. All data sets were indexed, integrated, and scaled with the HKL software, and for structural refinement, the Phenix suite was used.[18] Coot was used for visualizing the model and electron density.[19] Data collection statistics are listed in Table S1 of the Supporting Information. The crystal structure of FDR was deposited in the Protein Data Bank (PDB) as entry 4TPU.

RESULTS

Crystal Structure. The crystal structure of oxidized FDR from *M. acetivorans* was determined by single-wavelength anomalous diffraction (SAD) (PDB entry 4TPU). The crystal belonged to cubic space group *P*23. The 2.35 Å resolution structure refined to R_{cryst} and R_{free} values of 20.19 and 26.86%, respectively. A pair of 2-fold symmetry-related monomers forms a homodimer in which each of the N-terminal domains is in the proximity of the C-terminal domains of the other in a reciprocal fashion (Figure 1). Dynamic light scattering of the enzyme in solution confirmed the dimeric structure. A total of 16 hydrogen bonding interactions aid dimer formation. Eight such interactions on one side of the dimer are symmetrically repeated on the other side (Lys59 amino group with the Glu166 carboxyl group, Ile66, Pro68, and Leu63 carbonyls with the Arg167 guanidinium group, Ser20 and Lys19 side chains with the Ile160 carbonyl group, Arg122 guanidinium with the Arg170 carbonyl, and Lys134 amino group with the Lys134 carbonyl). The dimer is head to tail where the [Fe_4S_4] cluster of one monomer packs close to the [Fe_1S_0] center of the second monomer with the shortest distance between [Fe_4S_4] and [Fe_1S_0] being 12 Å (Figure 1 and Figure S1 of the Supporting Information).

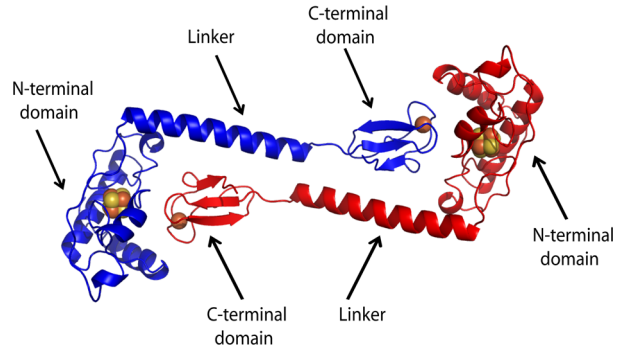

Figure 1. X-ray crystal structure of the FDR dimer. Each monomer shows the N-terminal domain with the Fe_4S_4 cluster, the C-terminal domain with the [Fe_1S_0] center, and the two domains linked by a helical linker. Dimer formation is aided by eight hydrogen bonding interactions on one side of the dimer that are symmetrically repeated on the other side (Lys59 amino group with the Glu166 carboxyl group, Ile66, Pro68, and Leu63 carbonyls with the Arg167 guanidinium group, Ser20 and Lys19 side chains with the Ile160 carbonyl group, Arg122 guanidinium with the Arg170 carbonyl group, and Lys134 amino group with the Lys134 carbonyl group).

DOI: 10.1021/acs.biochem.5b00137
Biochemistry 2015, 54, 3122−3128

The monomer is an elongated molecule (Figure 1) containing two domains linked by a 27-residue helix (109–135). The N-terminal domain of 104 residues consists of two long and three short α helices joined by loop regions. The overall structure is remarkably similar (root-mean-square deviation of 0.531 Å) to the catalytic subunit of the plant-type FTR with minor exceptions, which include the orientation of the FDR backbone from Val91 to the C-terminus (Figure S2 of the Supporting Information). The $[Fe_4S_4]$ cluster in FDR is situated close to the geometric center and 3.4 Å from a solvent-exposed Cys52/Cys84 disulfide (Figure S1 of the Supporting Information). This arrangement is nearly identical to the active site of FTR (Figure 2) in which the redox-active disulfide

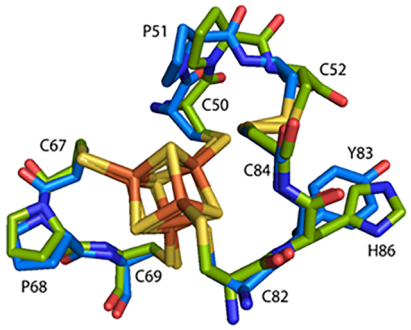

Figure 2. Superposition of the active sites of FDR and FTR. The backbone atoms of FDR are colored blue and those of FTR green. Residue numbering corresponds to FDR with the exception of His86 that belongs to FTR (PDB entry 1DJ7).

interacts with substrate (Figure S3 of the Supporting Information). Residues essential for the active-site architecture and mechanism of FTR are conserved in FDR (Figure 2 and Figure S4 of the Supporting Information), with the exception of Tyr83 replacing His86 of FTR, which is proposed to stabilize an essential intermediate in the postulated two-electron-reduced mechanism of catalysis (Figure S3 of the Supporting Information).[20]

Compared to that of FTR, the novel architecture of FDR resides in the C-terminal domain that contains 36 residues forming three antiparallel β strands (Figure 1). The linker and C-terminal domain have no structural resemblance or sequence identity to the variable subunit of FTR.[4,21] Instead, the C-terminal domain is similar in sequence and structure to bacterial-type rubredoxins (Figures S4 and S5 of the Supporting Information) and contains a rubredoxin-like $[Fe_1S_0]$ center coordinated to the sulfur atoms of Cys142, Cys145, Cys158, and Cys161 similar to bacterial-type rubredoxins (Figure S4 of the Supporting Information). In the dimer, the $[Fe_1S_0]$ center is positioned 12 Å from the side of the $[Fe_4S_4]$ cluster opposite the solvent-exposed disulfide (Figure S1 of the Supporting Information).

Biochemical Characterization. Metal analysis revealed 4.6 ± 0.1 Fe atoms per FDR monomer, consistent with one $[Fe_4S_4]$ cluster and one $[Fe_1S_0]$ center. The spectrum of anaerobically purified FDR (Figure 3) with an A_{max} of 425 nm is characteristic of the transient intermediate proposed for the mechanism of plant-type FTR (Figure S3 of the Supporting Information) in which the active-site disulfide is reduced and poised for interaction with substrate.[20,21] When the sample is exposed to air, the A_{max} of 425 nm of FDR shifted to 412 nm, characteristic of the oxidized $[Fe_4S_4]^{2+}$ resting state of FTR.[20]

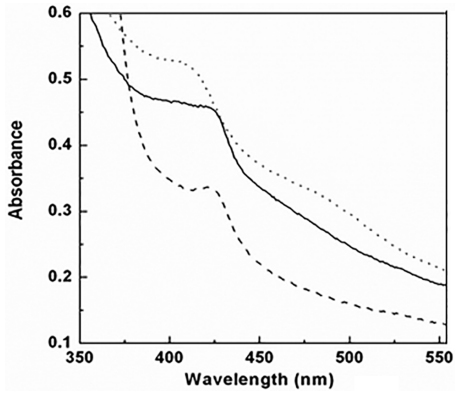

Figure 3. UV–visible spectra of anaerobically purified FDR. The concentration of FDR was 0.6 mM in 20 mM HEPES buffer (pH 7.5): (—) as purified, (···) air-oxidized, and (---) air-oxidized and reduced with dithionite.

The spectrum of air-oxidized FDR also showed absorbance at 485 nm typical of oxidized $[Fe_1S_0]^{3+}$ rubredoxin-like centers, indicating that the center was reduced in anaerobically purified FDR. Dithionite reduction of oxidized FDR yielded a spectrum resembling that of the anaerobically purified enzyme. Support for FDX as the electron donor to FDR is shown in Figure 4.

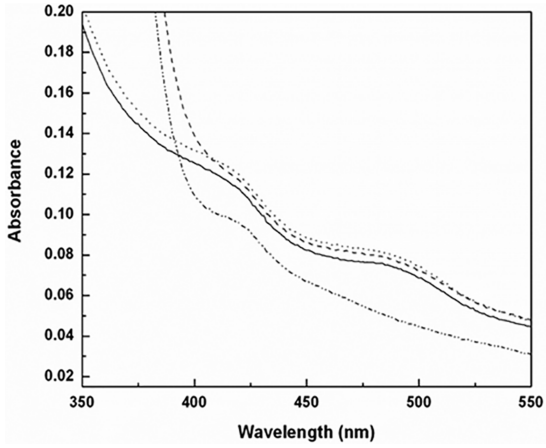

Figure 4. Ferredoxin-dependent reduction of air-oxidized FDR. The concentration of FDR was 0.15 mM: (—) oxidized FDR in 20 mM HEPES (pH 7.5), (···) further addition of 4.0 μM plant-type $[Fe_2S_2]$ FDX, (---) further addition of 0.1 mM NADPH, and (–·–) further and final addition of 0.1 unit of FNR. Substitution with 2$[Fe_4S_4]$ FDX from *M. acetivorans* produced identical results.

Reduction of oxidized FDR with the reduced FDX-regenerating system yielded the two-electron-reduced enzyme evidenced by a shift in absorbance A_{max} from 412 to 425 nm and a loss of absorbance at 485 nm resembling the anaerobically purified or dithionite-reduced enzyme. The plant-type FDX and the FDX from *M. acetivorans* were interchangeable.

The structural similarity of active sites between FDR and plant-type FTR suggested similar reaction mechanisms. Unlike FTR, the reduced form of FDR was stabilized, which facilitated an understanding of the mechanism. Indeed, the spectra of reduced FDR (Figures 3 and 4) suggested a catalytic intermediate analogous to the transient intermediate proposed for FTR (Figure S3 of the Supporting Information) in which the disulfide of FDR adjacent to $[Fe_4S_4]^{3+}$ is reduced, exposing the Cys52 thiol for interaction with the disulfide substrate and

DOI: 10.1021/acs.biochem.5b00137
Biochemistry 2015, 54, 3122–3128

producing a mixed disulfide intermediate available for reduction with a second electron from the $[Fe_1S_0]^{2+}$ center. Accordingly, it was expected that addition of substrate to reduced FDR would result in a single-turnover event returning the enzyme to the resting $[Fe_4S_4]^{2+}$ state identified by a spectral shift in A_{max} from 425 to 412 nm and the appearance of absorbance with an A_{max} of 485 nm indicating oxidation of $[Fe_1S_0]^{2+}$. Addition of thioredoxin from *E. coli*, or *M. acetivorans*, failed to perturb the spectrum like insulin did. The homo- and heterodisulfides of coenzymes M and B (HS-CoM and HS-CoB, respectively), essential for all methanogenic pathways, also failed to perturb the spectrum. However, the addition of glutathione (GSSG) to reduced FDR resulted in a spectral shift in A_{max} from 425 to 412 nm and the appearance of a broad peak centered at 485 nm indicating an oxidized $[Fe_1S_0]^{3+}$ center (Figure 5). The results

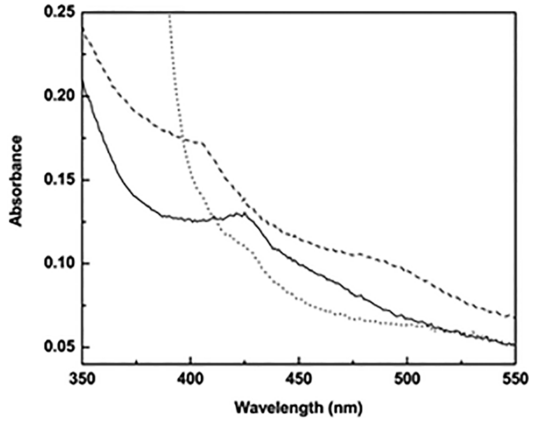

Figure 5. Effect of the addition of glutathione on the UV−visible spectrum of reduced FDR: (—) 0.18 mM anaerobically purified FDR in 20 mM HEPES (pH 7.5), (---) 1 mM GSSG added, and (···) FDR reduced with sodium dithionite after the addition of GSSG.

suggest a single-turnover event in which GSSG was reduced to GSH by mechanisms proposed for FTR (Figure S3 of the Supporting Information). Although the amount of GSH produced with a single turnover was below the limit of detection, turnover was confirmed when the sample was assayed upon addition of the *M. acetivorans* $2[Fe_4S_4]$ FDX regenerating system that produced 0.3 nmol of GSH min^{-1} $(mg\ of\ FDR)^{-1}$.

DISCUSSION

Bioinformatics analyses identified a family of diverse disulfide reductases that evolved from an ancestral plant-type FTR catalytic subunit to meet a variety of physiological requirements.[2] The results reported here represent the first structural and biochemical characterization of a member from this family, and the first FTR-like enzyme from methane-producing species of the domain Archaea.

Although interaction with GSSG established the disulfide reducing activity of FDR, GSSG is an unlikely physiological substrate. Genes encoding enzymes for the synthesis of GSSG are absent in the genome of *M. acetivorans*.[22] Furthermore, glutathione reductase was not detected in *Methanosarcina barkeri*, a close relative of *M. acetivorans*.[23] An improbable physiological role for GSSG is further reinforced by the rare occurrence in prokaryotes that instead utilize a diversity of sulfhydryl compounds as substitutes.[24] Finally, the rate of GSSG reduction [0.3 nmol min^{-1} $(mg\ of\ FDR)^{-1}$] is unlikely to be physiologically relevant and is near the limit of detection that also precluded reliable kinetic analyses. Although FDR failed to reduce the thioredoxins tested, the genome of *M. acetivorans* is annotated with seven homologues of which one or more may be specific for FDR.[25] It is also possible that reduction of the thioredoxin may be dependent on interaction of it with partner substrates. Finally, a variety of disulfide-containing proteins other than thioredoxin may be reduced by FDR for redox control, regulation of CO_2 fixation, and other functions as suggested previously.[2]

Proposed Mechanism. Although it is a likely fortuitous substrate, the reduction of GSSG by FDR in the anaerobically purified $[Fe_4S_4]^{3+}$ reduced state facilitated investigation of the mechanism. The results suggest a mechanism (Figure 6) analogous to the sequential one-electron-reduced mechanism proposed for FTR (Figure S3 of the Supporting Information).

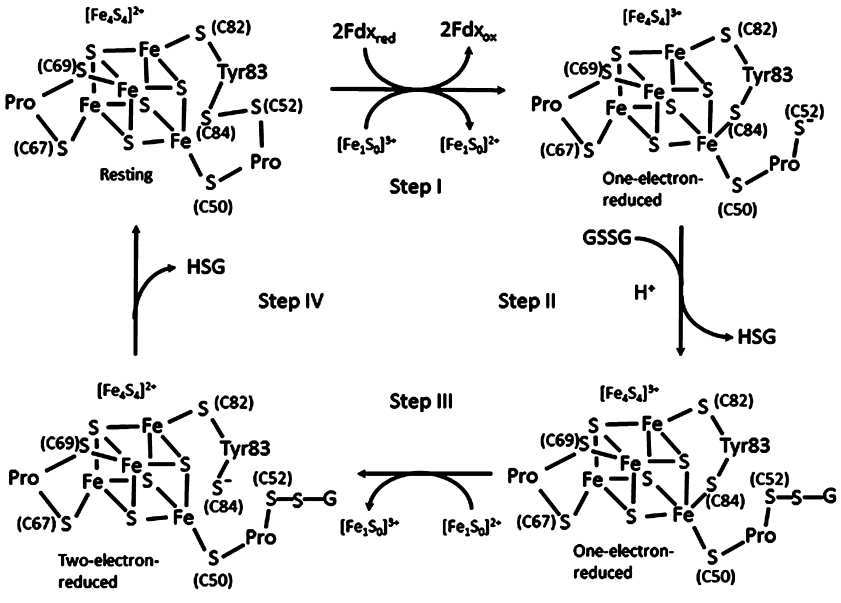

Figure 6. Mechanism proposed for FDR. Abbreviations: FDX_{red}, reduced FDX; FDX_{ox}, oxidized FDX.

DOI: 10.1021/acs.biochem.5b00137
Biochemistry 2015, 54, 3122−3128

In step I of the FDR mechanism, FDX donates an electron to the $[Fe_1S_0]^{3+}$ center that is transferred to the resting state $[Fe_4S_4]^{2+}$ cluster. A second electron from FDX regenerates a reduced $[Fe_1S_0]^{2+}$ center. The electron from FDX together with an electron from the resting state cluster reduces the adjacent Cys52/Cys84 disulfide, yielding the special five-coordinate Fe of the resulting $[Fe_4S_4]^{3+}$ cluster ligated to the sulfur of Cys84 that stabilizes a thiyl radical positioned on the sulfur atom of Cys52. It is this intermediate state that is reproduced when FDR is anaerobically purified or the air-oxidized enzyme is reduced with FDX. In step II, the thiyl radical of Cys52 attacks incoming GSSG, forming the $[Fe_4S_4]^{3+}$ mixed disulfide intermediate and releasing the first molecule of reduced glutathione (GSH). In step III, an electron from the reduced $[Fe_1S_0]^{2+}$ center is donated to the $[Fe_4S_4]^{3+}$ cluster, producing the $[Fe_4S_4]^{2+}$ mixed disulfide and the thiol of Cys84. Titration of air-oxidized FDR with dithionite revealed an initial loss of absorbance at 485 nm followed by a shift in A_{max} from 412 to 425 nm, a result further supporting a role for the $[Fe_1S_0]$ center in mediating the transfer of an electron from FDX to the $[Fe_4S_4]^{3+}$ cluster (Figure S6 of the Supporting Information). The finding that the reduced $[Fe_1S_0]^{2+}$ center is oxidized upon addition of GSSG to reduced FDR (Figure 5) is strong support for the proposed sequential one-electron-reduced mechanism. The final step IV involves disulfide exchange, producing the second molecule of GSH and the resting state of the enzyme containing the disulfide of the redox-active Cys52/Cys84 pair.

The $[Fe_1S_0]$ center is a potential entry point for the delivery of an electron to the $[Fe_4S_4]$ cluster for reduction of the Cys52/Cys84 disulfide. There are three possible electron transfer pathways with covalent or H-bonding connections between the $[Fe_1S_0]$ center and the $[Fe_4S_4]$ cluster in addition to a 12 Å through-space transfer (Figure 7). Although the biochemical and structural results are consistent with a role for the rubredoxin-like $[Fe_1S_0]^{2+}$ center in transfer of an electron to the $[Fe_4S_4]^{3+}$ mixed disulfide intermediate (Figure 6), redox potentials between −95 and 63 mV determined for rubredoxins[26] and −155 mV for the NEM-modified $[Fe_4S_4]^{3+}$ center of FTR[20] would appear to preclude efficient transfer. However, comprehensive spectroscopic analyses, including determination of redox potentials, are necessary to further investigate the proposed mechanism.

The mechanism proposed for FDR is analogous to the mechanism proposed for HDR (Figure S7 of the Supporting Information), a key enzyme in all pathways of methanogenesis catalyzing reduction of the heterodisulfide of coenzyme M and coenzyme B (CoM-S-S-CoB).[27] The primary difference between FDR and HDR is a direct attachment of HS-CoM to an iron in the active-site $[Fe_4S_4]^{3+}$ cluster of HDR, which is distinct from FDR in which the substrate interacts with the active-site cysteine disulfide. Nonetheless, the mechanisms proposed for FDR and HDR from methane-producing species involve redox chemistry and a novel $[Fe_4S_4]^{3+}$ cluster intermediate with two thiolate ligands bound at a unique iron in the cluster.

Support for the one-electron-reduced mechanism of FDR contrasts with that for an alternative mechanism proposed for the plant-type FTR in which substrate reacts with the two-electron-reduced enzyme containing $[Fe_4S_4]^{2+}$ and the reactive Cys57 thiol (Figure S3 of the Supporting Information).[20,27] The one-electron-reduced $[Fe_4S_4]^{3+}$ intermediate in FTR is transient and stabilized only by alkylation of Cys57 or replacement of this residue with serine.[3,20,28] Thus, stabilization

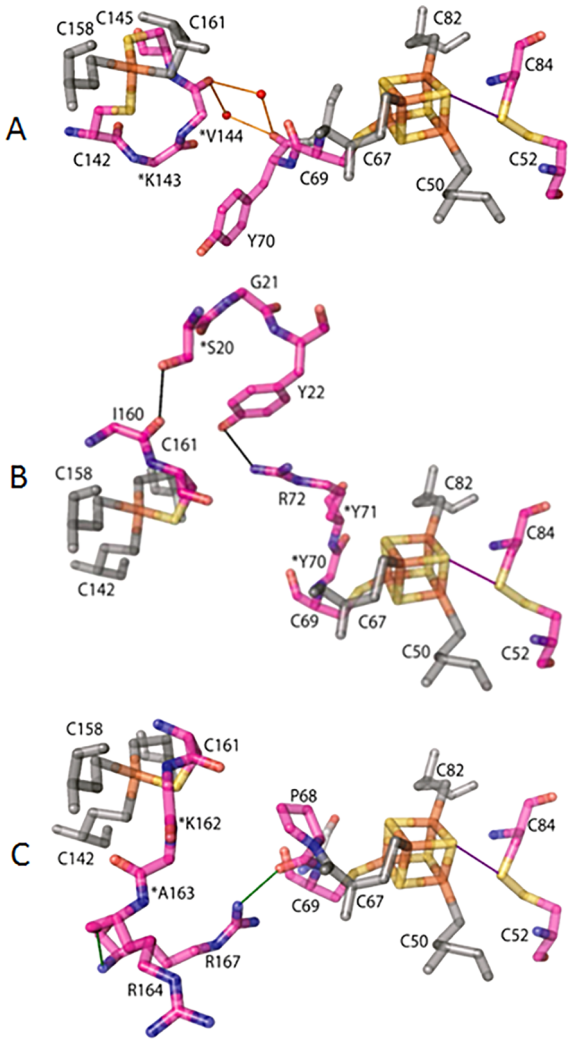

Figure 7. Active site of FDR showing three possible electron transport pathways from the $[Fe_1S_0]$ center to the Fe_4S_4 cluster. The first pathway (A) originates with Cys142 ligated to the $[Fe_1S_0]$ center with subsequent linkage through the backbone to the carbonyl of Val144 from where either of the two water molecules (red balls) that are within hydrogen bonding distances facilitate the transfer to the backbone carbonyl at Tyr70 and to the backbone of Cys69 ligating the $[Fe_4S_4]$ cluster. A second potential pathway (B) starts at Cys161 ligated to the $[Fe_1S_0]$ center, through to the backbone of Ile160, across the hydrogen bond to the side chain of Ser20 through the backbone of residue 21 to the side chain of Tyr22, across the hydrogen bond to the side chain of Arg72, and finally utilizing the backbone connection of residues 71 and 70 with Cys69 ligating the $[Fe_4S_4]$ cluster. The third pathway (C) also originates at Cys161 with sequential transfers through the backbone to the side chain of Arg164, across the hydrogen bond to the backbone amide of Arg167, through the hydrogen bond from the side chain of Arg167 to the backbone carbonyl of Pro68 and on to Cys69 ligating the $[Fe_4S_4]$ cluster. There could be a direct electron transfer from the $[Fe_4S_4]$ cluster to Cys84 of the Cys52/Cys84 disulfide as they are only 3.4 Å apart.

of the one-electron-reduced $[Fe_4S_4]^{3+}$ intermediate in FDR reacting with substrate strong supports the one-electron-reduced mechanism. In the FTR alternative mechanism (Figure S3 of the Supporting Information), His86 is proposed to play a role in stabilizing the two-electron intermediate by interaction with Cys87.[20] Replacement of His86 with Tyr greatly reduces the activity of FTR, which is consistent with the two-electron-

DOI: 10.1021/acs.biochem.5b00137
Biochemistry 2015, 54, 3122−3128

reduced mechanism.[20] Interestingly, Tyr83 in FDR is in a position nearly identical to that of His86 in FTR (Figure 2). Although a two-electron-reduced mechanism for FDR cannot be ruled out with certainty, the results presented here suggest an alternative role for Tyr83 in the proposed one-electron-reduced mechanism of FDR. A potential function for Tyr83 is to orient the thiolate anion of Cys84 for attack on the mixed disulfide in step IV of the proposed mechanism (Figure 6).

Evolutionary Considerations. The results support an essential role for the rubredoxin-like C-terminal domain in FDR and suggest a rationale for its evolution from the ancestral plant-type FTR catalytic subunit that was previously postulated.[2] The conserved regions (Figure S4 of the Supporting Information) and structure (Figure S2 of the Supporting Information) of the C-terminal domain closely resemble those of rubredoxins from the domain Bacteria, consistent with evolution of FDR solely via horizontal gene transfer in keeping with the proposal that *M. acetivorans* evolved at approximately the time of the end-Permian extinction and acquired numerous metabolic capabilities from the domain Bacteria.[5] The genome of *M. acetivorans* lacks annotations for rubredoxins other than those for FDR, suggesting rubredoxins are not of general importance in electron transport processes other than the function in FDR.

Several unique properties of FDR can be attributed to the C-terminal domain acquired via evolution from the ancestral FTR. First, FDR is stable to purification, consistent with the C-terminal domain and linker acting like the variable subunit required for stabilizing the catalytic subunit of FTR that is a requirement for purification of an active enzyme.[4] Second, reduction of FTR with dithionite requires methyl viologen as a mediator in contrast to FDR, which is reduced directly.[29] A plausible explanation for this difference rests on the ability of the $[Fe_1S_0]$ center of FDR to mediate the transfer of an electron from dithionite to the $[Fe_4S_4]$ cluster. In contrast to FTR,[20,30] the one-electron $[Fe_4S_4]^{3+}$ intermediate of FDR is stable, which can be explained by the reduced $[Fe_1S_0]^{2+}$ center protecting the reduced intermediate from oxidation.

Concluding Remarks. Bioinformatics analyses identified a family of diverse disulfide reductases that evolved from an ancestral plant-type FTR catalytic subunit to meet a variety of ecological needs.[2] The structural and biochemical characterization of the first representative from this family has initiated and advanced a structural, mechanistic, and evolutionary understanding of the family. Finally, the results provide an experimental foundation for identifying the substrates interacting with FDR that will reveal fundamental processes advancing a physiological understanding of methanogenic microbes.

■ ASSOCIATED CONTENT

Supporting Information

Materials and Methods, including methods for cloning, heterologous production, and purification of thioredoxin from *M. acetivorans*; a table of crystallographic data collection statistics; figures illustrating crystallographic properties, including a stereo image of the approximate protein contact potential, superposition of the FDR N-terminal domain with the FTR catalytic subunit, and structural comparison of FDR versus *Desulfovibrio vulgaris* rubredoxin; and additional figures, including a multiple-sequence alignment of FDR, FTR from *Synechocystis* sp. PCC 6803, and rubredoxin from *D. vulgaris*, titration of oxidized FDR with sodium dithionite, and mechanisms proposed for FDR and HDR. The Supporting Information is available free of charge on the ACS Publications website at DOI: 10.1021/acs.biochem.5b00137.

■ AUTHOR INFORMATION

Corresponding Authors

*Department of Biochemistry and Molecular Biology, Pennsylvania State University, University Park, PA 16802. E-mail: jgf3@psu.edu. Telephone: (814) 863-5721.

*Department of Biochemistry and Molecular Biology, Pennsylvania State University, University Park, PA 16802. E-mail: hpy1@psu.edu. Telephone: (814) 865-8383.

Present Address

§A.K.K.: Sardar Patel Renewable Energy Research Institute, Vallabh Vidyanagar, Anand 388120, Gujarat, India.

Author Contributions

A.K.K., R.S.S.K., and J.G.F. designed the research. A.K.K. and R.S.S.K. performed biochemical experiments. A.K.K., N.H.Y., and H.P.Y. performed crystallographic experiments and determined the crystal structure. A.K.K., H.P.Y., and J.G.F. wrote the paper; all authors helped with the final draft.

Funding

This work was supported by the Division of Chemical Sciences, Geosciences, and Biosciences, Office of Basic Energy Sciences, U.S. Department of Energy, via Contract DE-FG02-95ER20198 MOD16 awarded to J.G.F. National Institutes of Health-National Center for Research Resources Shared Instrumentation Grant 1S10RR023439-01 was awarded to N.H.Y. The National Science Foundation (NSF) and the National Institutes of Health via NSF Grant DMR-1332208 supported CHESS. National Institute of General Medical Sciences Grant GM-103485 supported MacCHESS.

Notes

The authors declare no competing financial interest.

■ ACKNOWLEDGMENTS

The CoM-S-S-CoB heterodisulfide was a gift of Jan Keltjens. *E. coli* thioredoxin was a gift from Biswarup Mukopadhyay. We thank B. Buchanan and P. Schurmann for helpful discussions. We wish to acknowledge help provided by the beam line staff at MacCHESS.

■ ABBREVIATIONS

CHESS, Cornell High Energy Synchrotron Source; CoMSH, coenzyme M; CoBSH, coenzyme B; FDR, ferredoxin:disulfide reductase; FTR, ferredoxin:thioredoxin reductase; FNR, ferredoxin:NADPH reductase; FDX, ferredoxin; GSSG, oxidized glutathione; GSH, reduced glutathione; HDR, heterodisulfide reductase; NEM, *N*-ethylmaleimide; SAD, single-wavelength anomalous diffraction.

■ REFERENCES

(1) Hanschmann, E. M., Godoy, J. R., Berndt, C., Hudemann, C., and Lillig, C. H. (2013) Thioredoxins, glutaredoxins, and peroxiredoxins. Molecular mechanisms and health significance: From cofactors to antioxidants to redox signaling. *Antioxid. Redox Signaling 19*, 1539–1605.

(2) Balsera, M., Uberegui, E., Susanti, D., Schmitz, R. A., Mukhopadhyay, B., Schurmann, P., and Buchanan, B. B. (2013) Ferredoxin:thioredoxin reductase (FTR) links the regulation of oxygenic photosynthesis to deeply rooted bacteria. *Planta 237*, 619–635.

DOI: 10.1021/acs.biochem.5b00137
Biochemistry 2015, 54, 3122–3128

(3) Walters, E. M., and Johnson, M. K. (2004) Ferredoxin:thioredoxin reductase: Disulfide reduction catalyzed *via* novel site-specific [4Fe-4S] cluster chemistry. *Photosynth. Res. 79*, 249−264.
(4) Jacquot, J. P., Eklund, H., Rouhier, N., and Schurmann, P. (2009) Structural and evolutionary aspects of thioredoxin reductases in photosynthetic organisms. *Trends Plant Sci. 14*, 336−343.
(5) Rothman, D. H., Fournier, G. P., French, K. L., Alm, E. J., Boyle, E. A., Cao, C., and Summons, R. E. (2014) Methanogenic burst in the end-Permian carbon cycle. *Proc. Natl. Acad. Sci. U.S.A. 111*, 5462−5467.
(6) Lee, D. Y., Ahn, B. Y., and Kim, K. S. (2000) A thioredoxin from the hyperthermophilic archaeon *Methanococcus jannaschii* has a glutaredoxin-like fold but thioredoxin-like activities. *Biochemistry 39*, 6652−6659.
(7) Amegbey, G. Y., Monzavi, H., Habibi-Nazhad, B., Bhattacharyya, S., and Wishart, D. S. (2003) Structural and functional characterization of a thioredoxin-like protein (Mt0807) from *Methanobacterium thermoautotrophicum*. *Biochemistry 42*, 8001−8010.
(8) Esposito, L., Ruggiero, A., Masullo, M., Ruocco, M. R., Lamberti, A., Arcari, P., Zagari, A., and Vitagliano, L. (2012) Crystallographic and spectroscopic characterizations of *Sulfolobus solfataricus* TrxA1 provide insights into the determinants of thioredoxin fold stability. *J. Struct. Biol. 177*, 506−512.
(9) Bhattacharyya, S., Habibi-Nazhad, B., Amegbey, G., Slupsky, C. M., Yee, A., Arrowsmith, C., and Wishart, D. S. (2002) Identification of a novel archaebacterial thioredoxin: Determination of function through structure. *Biochemistry 41*, 4760−4770.
(10) Susanti, D., Wong, J. H., Vensel, W. H., Loganathan, U., Desantis, R., Schmitz, R. A., Balsera, M., Buchanan, B. B., and Mukhopadhyay, B. (2014) Thioredoxin targets fundamental processes in a methane-producing archaeon, *Methanocaldococcus jannaschii*. *Proc. Natl. Acad. Sci. U.S.A. 111*, 2608−2613.
(11) Hernandez, H. H., Jaquez, O. A., Hamill, M. J., Elliott, S. J., and Drennan, C. L. (2008) Thioredoxin reductase from *Thermoplasma acidophilum*: A new twist on redox regulation. *Biochemistry 47*, 9728−9737.
(12) Kashima, Y., and Ishikawa, K. (2003) A hyperthermostable novel protein-disulfide oxidoreductase is reduced by thioredoxin reductase from hyperthermophilic archaeon *Pyrococcus horikoshii*. *Arch. Biochem. Biophys. 418*, 179−185.
(13) Jeon, S. J., and Ishikawa, K. (2002) Identification and characterization of thioredoxin and thioredoxin reductase from *Aeropyrum pernix* K1. *Eur. J. Biochem. 269*, 5423−5430.
(14) Kumar, A. K., Yennawar, N. H., Yennawar, H. P., and Ferry, J. G. (2011) Expression, purification, crystallization and preliminary X-ray crystallographic analysis of a novel plant-type ferredoxin/thioredoxin reductase-like protein from *Methanosarcina acetivorans*. *Acta Crystallogr. F67*, 775−778.
(15) Wang, M., Tomb, J. F., and Ferry, J. G. (2011) Electron transport in acetate-grown *Methanosarcina acetivorans*. *BMC Microbiol. 11*, 165.
(16) Eskelinen, S., Haikonen, M., and Raisanen, S. (1983) Ferene-S as the chromogen for serum iron determinations. *Scand. J. Clin. Lab. Invest. 43*, 453−455.
(17) Adams, P. D., Afonine, P. V., Bunkoczi, G., Chen, V. B., Davis, I. W., Echols, N., Headd, J. J., Hung, L. W., Kapral, G. J., Grosse-Kunstleve, R. W., McCoy, A. J., Moriarty, N. W., Oeffner, R., Read, R. J., Richardson, D. C., Richardson, J. S., Terwilliger, T. C., and Zwart, P. H. (2010) PHENIX: A comprehensive Python-based system for macromolecular structure solution. *Acta Crystallogr. D66*, 213−221.
(18) Otwinowski, Z., and Minor, W. (1997) Processing of X-ray diffraction data collected in oscillation mode. In *Methods in Enzymology* (Carter, C. W., Jr., and Sweet, R. M., Eds.) pp 307−326, Academic Press Inc., New York.
(19) Emsley, P., Lohkamp, B., Scott, W. G., and Cowtan, K. (2010) Features and development of Coot. *Acta Crystallogr. D66*, 486−501.
(20) Walters, E. M., Garcia-Serres, R., Naik, S. G., Bourquin, F., Glauser, D. A., Schurmann, P., Huynh, B. H., and Johnson, M. K. (2009) Role of histidine-86 in the catalytic mechanism of ferredoxin:thioredoxin reductase. *Biochemistry 48*, 1016−1024.
(21) Dai, S., Friemann, R., Glauser, D. A., Bourquin, F., Manieri, W., Schurmann, P., and Eklund, H. (2007) Structural snapshots along the reaction pathway of ferredoxin-thioredoxin reductase. *Nature 448*, 92−96.
(22) Galagan, J. E., Nusbaum, C., Roy, A., Endrizzi, M. G., Macdonald, P., FitzHugh, W., Calvo, S., Engels, R., Smirnov, S., Atnoor, D., Brown, A., Allen, N., Naylor, J., Stange-Thomann, N., DeArellano, K., Johnson, R., Linton, L., McEwan, P., McKernan, K., Talamas, J., Tirrell, A., Ye, W., Zimmer, A., Barber, R. D., Cann, I., Graham, D. E., Grahame, D. A., Guss, A. M., Hedderich, R., Ingram-Smith, C., Kuettner, H. C., Krzycki, J. A., Leigh, J. A., Li, W., Liu, J., Mukhopadhyay, B., Reeve, J. N., Smith, K., Springer, T. A., Umayam, L. A., White, O., White, R. H., de Macario, E. C., Ferry, J. G., Jarrell, K. F., Jing, H., Macario, A. J., Paulsen, I., Pritchett, M., Sowers, K. R., Swanson, R. V., Zinder, S. H., Lander, E., Metcalf, W. W., and Birren, B. (2002) The genome of *M. acetivorans* reveals extensive metabolic and physiological diversity. *Genome Res. 12*, 532−542.
(23) Ondarza, R. N., Rendon, J. L., and Ondarza, M. (1983) Glutathione reductase in evolution. *J. Mol. Evol. 19*, 371−375.
(24) Fahey, R. C. (2013) Glutathione analogs in prokaryotes. *Biochim. Biophys. Acta 1830*, 3182−3198.
(25) McCarver, A. C., and Lessner, D. J. (2014) Molecular characterization of the thioredoxin system from *Methanosarcina acetivorans*. *FEBS J. 281*, 4598−4611.
(26) Eidsness, M. K., Burden, A. E., Richie, K. A., Kurtz, D. M., Jr., Scott, R. A., Smith, E. T., Ichiye, T., Beard, B., Min, T., and Kang, C. (1999) Modulation of the redox potential of the $[Fe(SCys)_4]$ site in rubredoxin by the orientation of a peptide dipole. *Biochemistry 38*, 14803−14809.
(27) Walters, E. M., Garcia-Serres, R., Jameson, G. N., Glauser, D. A., Bourquin, F., Manieri, W., Schurmann, P., Johnson, M. K., and Huynh, B. H. (2005) Spectroscopic characterization of site-specific $[Fe_4S_4]$ cluster chemistry in ferredoxin:thioredoxin reductase: Implications for the catalytic mechanism. *J. Am. Chem. Soc. 127*, 9612−9624.
(28) Jameson, G. N., Walters, E. M., Manieri, W., Schurmann, P., Johnson, M. K., and Huynh, B. H. (2003) Spectroscopic evidence for site specific chemistry at a unique iron site of the [4Fe-4S] cluster in ferredoxin:thioredoxin reductase. *J. Am. Chem. Soc. 125*, 1146−1147.
(29) Schurmann, P., Stritt-Etter, A. L., and Li, J. (1995) Reduction of ferredoxin:thioredoxin reductase by artificial electron donors. *Photosynth. Res. 46*, 309−312.
(30) Glauser, D. A., Bourquin, F., Manieri, W., and Schurmann, P. (2004) Characterization of ferredoxin:thioredoxin reductase modified by site-directed mutagenesis. *J. Biol. Chem. 279*, 16662−16669.

DOI: 10.1021/acs.biochem.5b00137
Biochemistry 2015, 54, 3122−3128